Smart Bridge Sensing for Automated Vehicle Weight Estimation in Complex Traffic Scenarios

Dawid Piotrowski[1], Marcin Jasiński[1], Artur Nowoświat[1], Piotr Łaziński[1], Qian Chen[2], Tony Yang[2]

[1]Faculty of Civil Engineering, Silesian University of Technology, Poland
[2]Faculty of Applied Science, The University of British Columbia, Canada
dawid.piotrowski@polsl.pl, marcin.jasinski@polsl.pl, artur.nowoswiat@polsl.pl,
piotr.lazinski@polsl.pl, qian.chen@ubc.ca, yang@civil.ubc.ca

Abstract

Structural Health Monitoring (SHM) systems installed on bridges are increasingly being used to analyze traffic parameters. This includes estimating the gross vehicle weight and may be referred to as Weigh-in-Motion (WIM) methods. However, current research relies predominantly on numerical analyzes, whereas available field experiments are typically performed under quasi-controlled conditions. Such studies often assume that a single vehicle is moving along the predefined path at a known speed. In contrast, real-world traffic is inherently non-deterministic, often making it impossible to precisely define all initial conditions. This article presents the SHM system installed on a network arch bridge in Wolin, Poland. Strains induced by passing vehicles are measured using fiber-optic sensors based on Fiber Bragg Grating (FBG) technology. A neural network (NN) algorithm, whose architecture was optimized using Particle Swarm Optimization (PSO), is then used to estimate vehicle weight, with particular emphasis placed on robustness to traffic-related uncertainties. The system directly incorporates the structural specificity of the bridge and involves multi-gate weight estimations by strain values recorded by a minimal number of sensors. To evaluate the performance of the proposed approach, various tests were performed using real-world traffic experiments, involving multiple vehicles and varying speed. The system achieved a mean absolute percentage error of 4.6%, also for several vehicles on the bridge, complex traffic scenarios, and dynamic effects included.

Keywords –

Structural Health Monitoring; Bridge Weigh-in-Motion; Machine Learning

1 Introduction

Structural Health Monitoring (SHM) is currently one of the fastest growing fields, combining engineering, science, and information technology. These systems integrate various measurement techniques and are widely applied to different types of structures. In bridge engineering, SHM has been increasingly used to estimate road traffic load in the form of Weigh-In-Motion (WIM) systems. It should address the issues associated with the non-deterministic nature, uncertain positioning, and variety of traffic scenarios. The available studies in the literature confirm that WIM is still evolving and remains an important area of industrial research [1].

However, existing WIM applications are subject to several limitations. A significant part of studies are based solely on numerical analyzes [2], while available field experiments are often conducted under quasi-controlled or laboratory conditions [3], [4]. Consequently, this study extends the WIM method, demonstrating the possibility of utilizing the structural specificity of the bridge and allowing the number of sensors required to be reduced. Furthermore, by using three independent measurement gates, the proposed method enables the determination of vehicle weight under unconstrained traffic conditions. The presented approach is resistant to random impact of multiple vehicles and dynamic effects while maintaining a high level of accuracy.

2 Literature review

In many cases, experiments assume the exact position and speed of the vehicle [5], [6]. In reality, traffic flow is inherently random, and therefore the results of such studies may not be fully representative of real-world traffic conditions. For example, Brzozowski et al. [7] investigated the influence of various external factors on the accuracy of weight estimates. Their results show that the vehicle traffic path is one of the most significant contributors to measurement error. For lateral load displacements of up to 50 cm, the total weight prediction error was approximately 10%, while for displacements exceeding 170 cm, the error increased dramatically to almost 30%.

Furthermore, many current WIM solutions require the definition of specific preconditions [8],[9], distributed measurements, or a large number of sensors, especially the influence line-based applications [10]-[13]. Although a higher level of accuracy can be achieved, the requirement to define input parameters such as the number, spacing of axles, or vehicle speed is often difficult to satisfy in real-world traffic. Moghadam [14] presented an example of the Nothing-on-Road (NOR) WIM application, which assumes the time delay between the strain peaks caused by the traversing axles. The study was conducted using numerical data under controlled conditions. Similarly, Wang et al. [15] proposed a method to estimate vehicle parameters using the vehicle-bridge interaction. In this approach, additional input data was defined in the form of roughness of the road surface, which was estimated using a particle filter. Moreover, the analysis was limited to two-axle vehicles and scenarios involving only a single vehicle. Under these assumptions, the maximum weight estimation error was 11.9%.

Consequently, WIM methods still lack experimental validation in which vehicle position, speed, and traffic composition are not known a priori. The method shown in this paper estimates vehicle weight in unconstrained traffic using three independent measurement gates and a limited number of sensors, while remaining accuracy in random multi-vehicle scenarios.

3 Methodology

3.1 Bridge case study description

This study introduces an SHM system installed on a network arch bridge in Wolin, Poland, in which one of the objectives is the detection of the gross weight of vehicles. The bridge analyzed is a steel structure with a theoretical span of 165.0 m. Its total width is 16.9 m and the height of the arch is 24.0 m (Figure 1).

3.2 System description

The system consists of a network of sensors in which data is acquired and processed using Machine Learning (ML) algorithms. The specificity of the bridge influenced the selection of the sensors, as the most significant feature of the structure is the local nature of the influence area of the crossbeams. Consequently, the increase in the strain in the crossbeams is specifically caused by vehicles located in their immediate vicinity. This ensures that the readings are not affected by vehicles farther away. To improve the robustness of the system and reduce the probability of two vehicles moving side by side in two lanes at the same, three consecutive measurement gates, each consisting of three sensors, are designed, located at 1/4, 1/2, and 3/4 of the span. This configuration allows for estimation of vehicle weight by three independent measurements recorded in different places along the bridge. The network is supplemented with two additional sensors located in the middle of the tie-beams. (Figure 2).

Figure 1. Analyzed arch bridge in Wolin, Poland

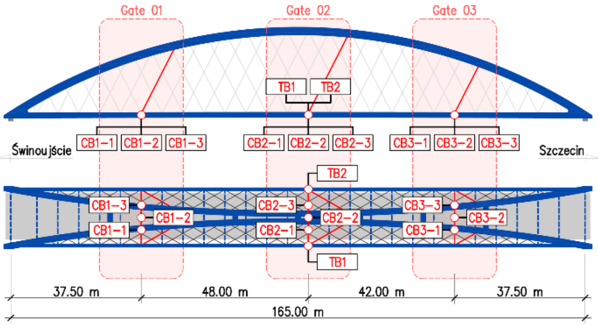

Figure 2. Distribution of the sensors on the bridge

The sensors were spot-welded directly to the surface of the element after the paint layer had been ground off. The sensors on the crossbeams are placed on the top surface of the bottom flange, whereas those on the tie-beams are installed underside of the section. The sensors were subsequently protected against corrosion using a non-hardening, high-adhesion masking sealant. Finally, they were covered with a 0.05 mm thick aluminum foil coated with a 3 mm layer of kneadable putty (Figure 3). The system enables synchronous acquisition of data from all channels allowing for time-correlation analysis.

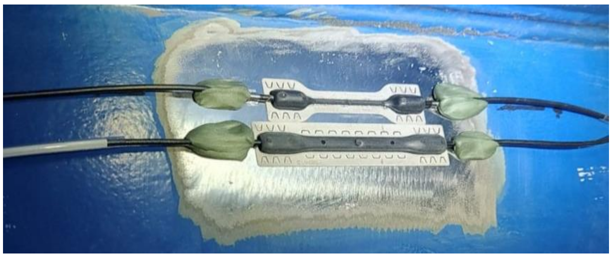

Figure 3. Example configuration of the sensor

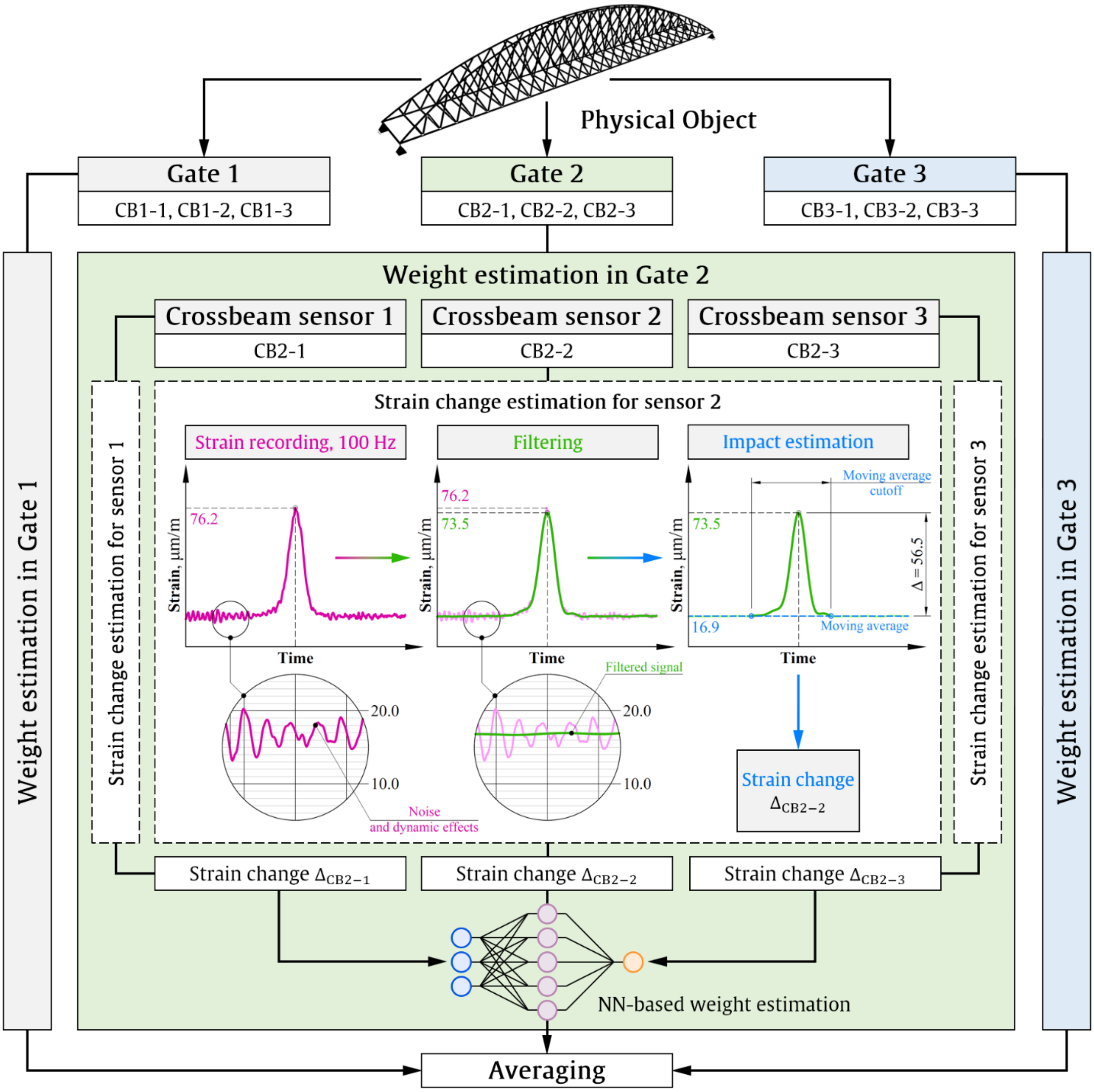

Figure 4. Overview of the proposed weight estimation methodology

The overview of the weight estimation methodology is shown in Figure 4. Each of the nine sensors records the strain with a frequency of 100 Hz. The time-series data are processed by an Infinite Impulse Response (IIR) Butterworth filter. It applies the low-pass design and processes the signal forward and backward to achieve zero-phase distortion. Using the processed signal, the moving average is calculated for each of the sensors independently, excluding outliers that usually indicate the beginning of the load impact. The moving average serves as a base against which the maximum strain value is compared to estimate the strain change due to vehicular load. The strain increases recorded by the sensors are grouped by timestamp and gate and, as such, are passed to the neural networks for weight estimation.

The proposed design incorporates three independent neural networks, each assigned to the specific gate and consisting of three input units. The networks are trained using data obtained through Finite Element (FE) simulation. An important part of the current procedure is an updated bridge FE model, calibrated on the basis of the static load test results. It involved minimization of the difference between the measured and simulated response, including strains and deflections due to a known and precisely arranged load.

The procedure of the FE model calibration involved the results of static load tests with nine trucks positioned in various scenarios, including three loading schemes above each of the measurement gates, individually, and two asymmetrical cases with trucks aligned to the left and right edges of the road. A Genetic Algorithm (GA) was applied, with the objective of minimizing the difference between the strains measured by the SHM system and those predicted by the FE model. The GA consisted of 20 generations of 150 candidates and reached convergence in the last generations. The input parameters of the GA were the elastic moduli of all structural elements with the assumed limit values of 160 – 240 GPa for steel and 5 – 45 GPa for concrete elements. Although the elastic moduli boundaries include values that exceed the standard values for structural steel and concrete, it was assumed that they should reflect different factors that affect the overall stiffness. The effects in question may include, but are not limited to, assembly clearances, inaccuracies in geometrical, material, and structural properties, and stiffness of the non-structural elements like pavement, caps, curbs, barriers or railings.

3.3 Optimization of the NN architecture

Choosing an appropriate neural network architecture is crucial to achieving high accuracy in estimating the gross weight of vehicles. This process involves defining the number of layers, the number of neurons in each layer, the activation function, and the learning rate, and can be formulated as a classical optimization task.

One of the most widely used optimization algorithms is the Particle Swarm Optimization (PSO), which is inspired by the behavior of a herd of animals cooperating to find an optimal solution. In PSO, a population of particles iteratively moves through the solution space, adjusting their position based on their individual best experience and the best position in the entire swarm.

Adopting appropriate values for the coefficients and inertia weight is a crucial element of the PSO algorithm and directly influences the accuracy of the results obtained. In order to balance global exploration and local exploitation, the inertia weight ω was dynamically updated at each iteration of the algorithm (Equation (1)).

$$\omega^{t+1} = \omega_{\max} - \left(\frac{\omega_{\max} - \omega_{\min}}{t_{\max}}\right) \cdot t \tag{1}$$

where, t_{max} denotes the maximum number of iterations, and t the current iteration. The inertia weight value was assumed in the range between of $\omega_{\min} = 0.4$ and $\omega_{\max} = 0.9$.

To determine the appropriate NN architecture for weight prediction, each PSO particle was represented in a 5-dimensional solution space. This consisted of: the number of layers ranging from 1 to 5, the number of neurons in the first hidden layer, the reduction factor for number of neurons applied to subsequent layers, the learning rate, and the activation function used, encoded in the numerical form: 0: ReLU, 1: leaky ReLU, 2: sigmoid, 3: hyperbolic tangent, 3: ELU, 4: SELU, 5: GELU, and 6: Swish.

The architectural search space was constrained to improve stability and reduce computational cost. The number of neurons in the first hidden layer was selected from a discrete set of powers of two from 32 to 256. The second parameter determining the number of neurons in subsequent layers was the reduction factor α. Instead of directly optimizing the reduction factor, an unconstrained auxiliary variable z was used in the PSO and then mapped to the admissible range via the sigmoid transformation (Equation (2)).

$$\alpha = 0.4 + 0.45 * \mathrm{sigmoid}(z) \tag{2}$$

Applying such a transformation results in a reduction factor ranging from 0.40 to 0.85 and ensures smooth exploration of the entire solution space. Additionally, layers with a small number of neurons destabilize the gradient propagation and increase the variance of the results, therefore a soft architectural regularization was used. For each particle in which a given hidden layer had fewer than 16 neurons, the Root Mean Square Error (RMSE) value was increased by a relative penalty l proportional to both the current prediction error and the deviation from the minimum layer width (Equation (3)).

$$l = 0.2 \cdot \mathrm{RMSE} \cdot \frac{16 - n}{16} \tag{3}$$

where n is the number of neurons in the hidden layer.

The learning rate was optimized in the logarithmic domain, with the search space defined between $\log_{10}(0.0005)$ and $\log_{10}(0.1)$ which reflects the multiplicative nature of the learning rate and allows the algorithm to explore different orders of magnitude in a balanced manner. The final NN architectures and their RMSE obtained on the FE-sourced test set are presented in Table 1.

Table 1. NN architecture after PSO algorithm

Gate	**Number of layers**	Reducing factor	1st layer	2nd layer	3rd layer	4th layer	5th layer	Learning rate	Activation function	RMSE (kg)
1	4	0.8483	256	217	184	156	–	0.0008	GELU	97.0
2	3	0.5720	256	146	84	–	–	0.0119	GELU	115.3
3	4	0.6896	128	88	61	42	–	0.0061	Swish	110.8

4 Results

The accuracy of the system has been verified using vehicles of known weights and different configurations of axles, passing the bridge in various scenarios. The basic scenario, representing the target traffic conditions expected during the operational phase and detailed in Section 3.1, consists of a single truck passing the bridge in the left or right lane. Exemplary passages of multiple trucks and involving varying speed are presented in Sections 3.2 and 3.3, respectively.

4.1 Single-truck runs

The single-truck tests involved nine types of vehicles with gross weights in the range between 27.8 t and 41.5 t and a wheel arrangement including 3 to 6 axles (Table 2). Figure 5 shows the strain change in consecutive gates during a run of a 4-axle truck of 32.7 t total weight. The vehicle moves in the direction of the target traffic, first passing through Gate 3, then Gate 2, and finally Gate 1. The most significant strain increase is observed in the middle sensors, CB1-2, CB2-2, and CB3-2, in Gates 1, 2, and 3, respectively. The magnitude of strain increase in the outer sensors is consistent in all three gates and indicates the pass of the truck on the lane by side of the sensors labeled CB1-3, CB2-3, and CB3-3. The gross vehicle weight is independently estimated by each gate, resulting with values 34.4 t in Gate 1, 33.8 t in Gate 2, 33.4 t in Gate 3, and the average of 33.9 t (error: 3.5%).

The results of the rest of the single-truck runs, 18 in total, and the mean performance metrics of the system are given in Table 2. The mean absolute percentage error of 4.6% and respective mean absolute error of 1.5 t is achieved in the given scenarios, while maintaining the mean percentage error of –2.6% and the mean error of 0.7 t when considering the sign of predictions against the true values. Two tests out of the performed ones, namely the 6-axle truck of 41.4 t in the right lane and the 3-axle truck of 28.7 t in the left lane, are clearly outstanding. This kind of effect can be accounted for additional uncertainties related to transversal positioning of vehicles, axle configuration, and the overall impact of the axles spacing compared to the range of the influence area.

Table 2. Weight estimation and performance metrics in single-truck tests: ACC – Accuracy, MPE – Mean Percentage Error, MAPE – Mean Absolute Percentage Error, ME – Mean Error, MAE – Mean Absolute Error

Vehicle	Lane	**Weight estimation**, w				**Metrics**				
		Gate 1 (t)	Gate 2 (t)	Gate 3 (t)	**Average**, w_{mean} (t)	ACC (–)	MPE (%)	MAPE (%)	ME (t)	MAE (t)
6-axle	Right	37.1	37.4	37.2	37.2	0.899	10.13	10.13	–4.2	4.2
[**41.4 t**]	Left	39.9	41.3	41.5	40.9	0.986	1.353	1.353	–0.6	0.6
5-axle	Right	39.8	39.9	39.2	39.6	0.976	2.379	2.379	–1.0	1.0
[**40.6 t**]	Left	43.2	39.6	42.2	41.7	1.026	–2.625	2.625	1.1	1.1
5-axle	Right	39.4	40.1	39.8	39.8	0.958	4.224	4.224	–1.8	1.8
[**41.5 t**]	Left	42.7	41.7	42.9	42.4	1.022	–2.213	2.213	0.9	0.9
4-axle	Right	34.4	34.2	33.7	34.1	1.031	–3.097	3.097	1.0	1.0
[**33.0 t**]	Left	36.2	31.9	32.8	33.6	1.017	–1.702	1.702	0.6	0.6
4-axle	Right	33.2	33.1	32.4	32.9	1.023	–2.335	2.335	0.8	0.8
[**32.2 t**]	Left	34.0	32.1	32.7	32.9	1.024	–2.393	2.393	0.8	0.8
4-axle	Right	34.4	33.8	33.4	33.9	1.035	–3.516	3.516	1.2	1.2
[**32.7 t**]	Left	34.3	34.1	32.5	33.6	1.028	–2.805	2.805	0.9	0.9
3-axle	Right	31.9	30.9	30.8	31.2	1.088	–8.777	8.777	2.5	2.5
[**28.7 t**]	Left	33.4	34.8	31.7	33.3	1.161	–16.14	16.14	4.6	4.6
3-axle	Right	30.2	29.5	30.1	29.9	1.078	–7.813	7.813	2.2	2.2
[**27.8 t**]	Left	27.7	28.4	31.4	29.2	1.052	–5.191	5.191	1.4	1.4
3-axle	Right	30.3	30.7	30.7	30.6	1.062	–6.245	6.245	1.8	1.8
[**28.8 t**]	Left	28.8	29.1	28.4	28.8	0.999	0.061	0.061	0.0	0.0
					Mean:	1.026	–2.595	4.611	0.7	1.5
					Standard deviation:	0.056	5.567	3.951	1.8	1.2

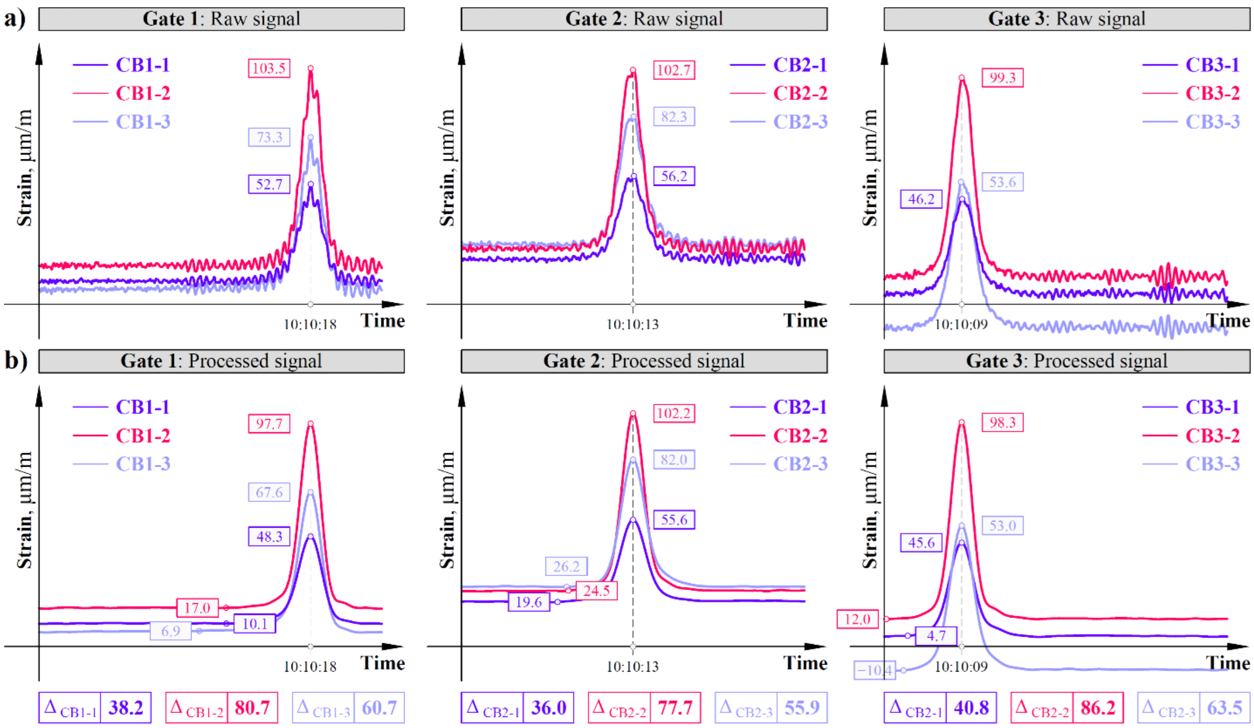

Figure 5. Exemplary strain change in a single-vehicle test in three consecutive measurement gates: a) raw signal, b) filtered signal, moving average, and the respective strain change

4.2 Multiple-truck runs

Although still relatively rare, the system should be resistant to vehicles arranged in groups and crossing the bridge in a convoy. To measure accuracy in this kind of scenarios, several tests were performed, among which the passage of 4-axle trucks of gross weights 33.0 t, 32.2 t and 32.7 t in the right lane was reported in the paper. The overview of the raw and filtered signals is shown in Figure 6. The performance of the system maintains the desired accuracy given by the MPE of –2.2%, MAPE of 2.2%, and both ME and MAE of 0.7 t, despite the clear overlapping of the second and third impacts. Thanks to the reduced range of the influence surface for crossbeam strains, relatively close vehicles can be separated and estimated with no additional measures, just due to the structural specificity of network arch bridges. The weight estimations reported for the three trucks in the test convoy are given in Table 3.

4.3 Runs of varying speed

Considering that specific applications are prone to the varying speed of vehicles, including the influence line-based ones, the given approach is evaluated against different velocities of trucks passing the bridge. An integral part of field tests is the vehicle moving at a speed of 30 km/h through an artificial obstacle, in this case a transversal step on the carriageway. In the given context, the step allows inducing additional dynamic excitations

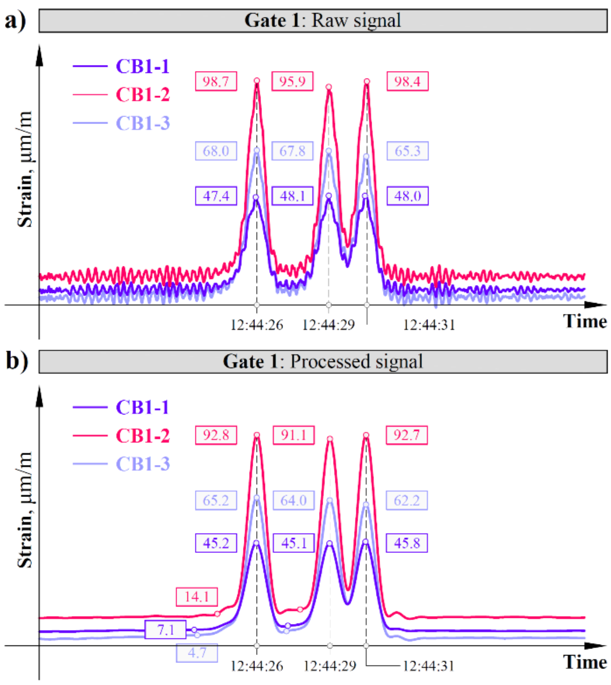

Figure 6. Exemplary strain change in a multiple-vehicle test in the Gate 1: a) raw signal, b) filtered signal

and signal disturbance and evaluate the system against unpredictable side-effects. The tests performed, among which the passage of the 4-axle truck in the left lane is reported in the paper, indicate the consistent performance in varying speed conditions. In Figure 7, compared to Figure 5, the strain increase in the sensors CB1-1 and CB1-2 in Gate 1, CB-2-1 and CB2-2 in Gate 2, and CB3-1 and CB3-2 in Gate 3 are alike, indicating the placement of the vehicle being away from the CB1-3, CB2-3, and CB3-3 sensors in the consecutive gates. One should note the distinctive signal artifacts in the 30 km/h passage with the artificial step mounted right above the gate. Despite the perturbations, the filter is able to reduce additional effects, and produce clear enough signal for further processing by the neural network.

Table 4 and Figure 7 report gross vehicle weights for varying passage velocities, indicating consistent results given by MPE of –0.8%, MAPE of 2.9%, ME of 0.3 t, and MAE of 0.9 t. Based on the results, the presented approach allows for achieving good estimation accuracy regardless of the accompanying dynamic effects and variations in vehicle type.

Table 3. Weight estimation and performance metrics in multiple-truck tests, 4-axle vehicles in the right lane

Vehicle	**Lane**	Gate 1 (t)	Gate 2 (t)	Gate 3 (t)	**Average**, w_{mean} (t)	ACC (–)	MPE (%)	MAPE (%)	ME (t)	MAE (t)
		Weight estimation, w				**Metrics**				
[**33.0 t**]	Right	34.7	33.9	33.8	34.1	1.033	–3.309	3.309	1.1	1.1
[**32.2 t**]	Right	32.9	31.1	34.3	32.8	1.019	–1.886	1.886	0.6	0.6
[**32.7 t**]	Right	32.3	32.0	35.3	33.2	1.015	–1.467	1.467	0.5	0.5
					Mean:	1.022	–2.221	2.221	0.7	0.7

Table 4. Weight estimation and performance metrics for varying velocities, gross vehicle weight of 32.7 t

Vehicle	**Lane**	Gate 1 (t)	Gate 2 (t)	Gate 3 (t)	**Average**, w_{mean} (t)	ACC (–)	MPE (%)	MAPE (%)	ME (t)	MAE (t)
		Weight estimation, w				**Metrics**				
30 km/h	Left	34.2	34.1	33.0	33.8	1.032	–3.199	3.199	1.0	1.0
50 km/h	Left	32.4	31.5	31.7	31.9	0.974	2.608	2.608	–0.9	0.9
80 km/h	Left	34.3	34.1	32.5	33.6	1.028	–2.791	2.791	0.9	0.9
					Mean:	1.008	–0.788	2.865	0.3	0.9

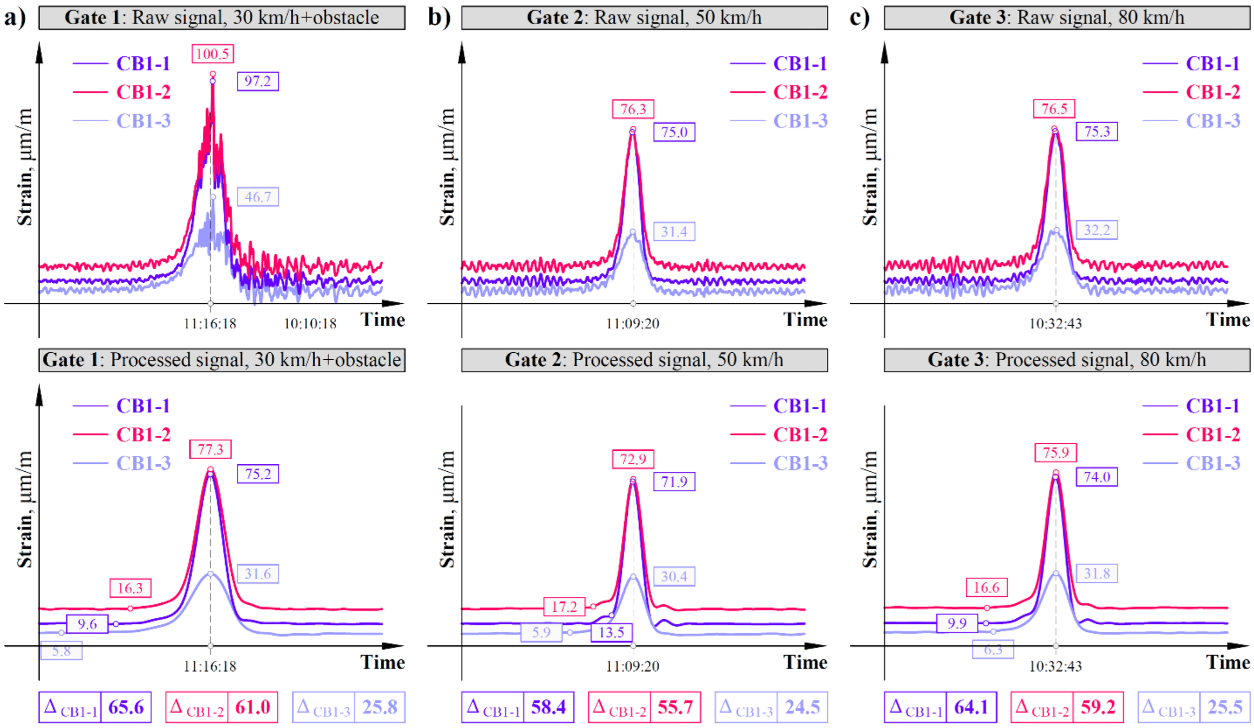

Figure 7. Exemplary strain change in a single-vehicle test for different passage velocities : a) 30 km/h with the dynamic impact due to artificial obstacle, b) 50 km/h, c) 80 km/h

5 Limitations

The proposed WIM approach constitutes a promising solution for long-term bridge monitoring under realistic traffic conditions, however several aspects may benefit from further investigation. The current validation was conducted on a single bridge structure, and future work will focus on extending the methodology to other bridge types. In addition, the neural networks were trained using data from a calibrated finite element model, which proved effective but could be further enhanced with larger datasets obtained directly from field measurements.

Moreover, although a range of vehicle configurations was considered, expanding the dataset may further improve the robustness of the model. These aspects do not affect the overall applicability of the method but rather indicate its potential for further development.

6 Conclusions

This research integrates the bridge SHM system using FBG sensors and ML to estimate the gross vehicle weight in real-word traffic. Unlike many existing WIM studies, the proposed approach was experimentally validated under realistic traffic conditions, without requiring prior knowledge of vehicle path or speed as input to the estimation algorithm.

The system achieved an average MAPE of 4.6% for single-vehicle run and 2.2% for multiple-vehicle runs, confirming its robustness to varying traffic scenarios. Moreover, the influence of vehicle speed and dynamic effects was shown to be limited and did not significantly degrade the prediction accuracy.

A key feature of the proposed methodology is the use of three independent measurement gates distributed along the span. The structural features of the network arch bridge, primarily the short-range influence area of the crossbeam strain, proved to beneficial in separating closely spaced vehicles, constituting an important component of the framework.

References

[1] D. Paul, K. Roy. Application of bridge weigh-in-motion system in bridge health monitoring: a state-of-the-art review. *Structural Health Monitoring*, 22(6):4194-4232 (2023).

[2] X. Xiao, D. Pi, Q. Zhu. A bridge weigh-in-motion algorithm for fast-passing railway freight vehicles considering bridge-vehicle interaction. *Mechanical Systems and Signal Processing*, 181 (2022) 109493

[3] S. Alamandala, R.L.N. Sai Prasad, Rathish Kumar Pancharathi et al. Study on bridge weigh in motion (BWIM) system for measuring the vehicle parameters based on strain measurement using FBG sensors. *Optical Fiber Technology*, 61 (2021) 102440.

[4] W. He, T. Ling, E. O'Brien et al. Virtual Axle Method for Bridge Weigh-in-Motion Systems Requiring No Axle Detector. *Journal of Bridge Engineering*, 24(9) 2019.

[5] C. Tan, B. Zhang, H. Zhao et al. An Extended Bridge Weigh-in-Motion System without Vehicular Axles and Speed Detectors Using Nonnegative LASSO Regularization. *Journal of Bridge Engineering*, 28(5) 2023.

[6] N. Zolghadri, M. W. Halling, N. Johnson et al. Field Verification of Simplified Bridge Weigh-in-Motion Techniques. *Journal of Bridge Engineering*, 21(10) 2016.

[7] K. Brzozowski, A. Maczyński, A. Ryguła, T. Konior. A weigh-in-motion system with automatic data reliability estimation. *Measurement*, 221 (2023) 113494.

[8] X. Jian, Y. Xia, S. Sun et al. Integrating bridge influence surface and computer vision for bridge weigh-in-motion in complicated traffic scenarios. *Structural Control and Health Monitoring*, 2022, 29

[9] L. Zhang, S. Wang, L. Deng et al. A general solution to bridge weigh-in-motion equations based on maximum likelihood estimation. *Engineering Structures*, 343 (2025), 121193

[10] A. J. Ferguson, D. Hester, F. Huseynov et al. On the normalisation and mapping of influence lines. *Mechanical Systems and Signal Processing*, 237, 112883 (2025)

[11] W. He, J. Liu, S. Song et al. A non-contact vehicle weighing approach based on bridge weigh-in-motion framework and computer vision techniques. *Measurement*, 225, 113994 (2024)

[12] H. Wu, H. Zhao, J. Liu et al. A filtering-based bridge weigh-in-motion system on a continuous multi-girder bridge considering the influence lines of different lanes. *Frontiers of Structural and Civil Engineering*, 14:1232-1246 (2020)

[13] I. Yoshida, S. Mustafa, K. Maruyama et al. Bridge weigh-in-motion considering dynamic response in observation noise with application to multiple driving conditions. *Structural Safety*, 103, 102350 (2023)

[14] A. Moghadam. A novel speed-adaptive framework for structural load evaluation using notihing-on-road bridge weigh-in-motion. *Structures*, 82 (2025) 110714.

[15] H. Wang, T. Nagayama, B. Zhao, D. Su. Identification of moving vehicle parameters using bridge responses and estimated bridge pavement roughness. *Engineering Structures*, 153:57-70, 2017.